Electrostatic waves in an electron-beam plasma system

Quanming Lu, Shui Wang, and Xiankang Dou
School of Earth and Space Sciences, University of Science and Technology of China, Hefei, Anhui 230026, People's Republic of China

(Received 21 January 2005; accepted 24 May 2005; published online 1 July 2005)

A one-dimensional (1D) electrostatic particle-in-cell simulation was performed to study wave excitation processes due to a tenuous electron beam in a plasma system, which is composed of hot and cold electron components. In this case, three types of electrostatic waves are excited, namely, Langmuir waves, electron-acoustic waves, and beam-driven waves. The beam-driven waves have a broad frequency spectrum, which extends from $(0.1-0.2)\omega_{pe}$ (ω_{pe} is the electron plasma frequency) to $(1.5-2.5)\omega_{pe}$, with phase speeds close to the speed of the electron beam. The interactions among these waves are investigated for different values of density, temperature, and speed of the electron beam, etc. One special case is that when the density of the electron beam is sufficiently high, compressive solitary waves with bipolar structure of the electric field are generated. The generation mechanism of these solitons is mainly due to the trapping of a fraction of the beam electrons by the potential well of the enhanced beam-driven waves, as shown by the holes that are formed in phase-space plots. The relevance of these excited electrostatic waves to the intense broadband electrostatic noise observed in the Earth's auroral region is also discussed. © *2005 American Institute of Physics*. [DOI: 10.1063/1.1951367]

I. INTRODUCTION

The electron-acoustic waves may be unstable in plasma composed of two electron components with different temperatures.[1–4] The existence of the electron-acoustic mode was first conceived when Fried and Gould[5] studied numerical solutions of the electrostatic dispersion equation in an unmagnetized, homogeneous plasma. They showed that, in addition to the well-known Langmuir and ion-acoustic waves, there exists another heavily damped acousticlike mode. It was later found that in the presence of two distinct components (cold and hot) of electrons, this wave mode is weakly damped. This mode is known as the electron-acoustic waves, which have properties significantly different from those of Langmuir waves.[6] Gary and Tokar[7] performed a parameter survey and found conditions for the existence of the electron-acoustic waves: the hot to cold electron temperature ratio is larger than ~10, and the hot electron component constitutes a non-negligible fraction of the total electron density (more than ~20%). The dispersion relation of the electron-acoustic mode in such a plasma system is given by[7]

$$\omega^2 = \omega_{pc}^2 \frac{1 + 3k^2\lambda_{Dc}^2}{1 + 1/(k^2\lambda_{Dh}^2)}, \tag{1}$$

where $\lambda_{Dc,h}=\sqrt{\varepsilon_0 k_B T_{c,h}/n_{c,h0}e^2}$ are the cold and hot electron Debye lengths ($T_{c,h}$ and $n_{c,h0}$ are the temperatures and densities of the background cold and hot electrons, respectively), $\omega_{pc}=\sqrt{n_{c0}e^2/m_e\varepsilon_0}$ is the plasma frequency of the cold electron component, ω is the wave frequency, and k is the wave number. The nonlinear evolution of electron-acoustic waves has also been studied with the Korteweg–de Vries (KdV) or modified KdV equation. The electron-acoustic waves may evolve into solitons when their amplitudes are sufficiently large. The potential structures of these solitons take the form of negative electrostatic pulses.[8–10]

It is known that a plasma system with two-electron components often occurs in the Earth's auroral region. In such a region, the cold electrons originate from the ionosphere (with temperature of ~1 eV), while the hot electrons (with temperature of ~100 eV) come from the magnetosphere. In addition to these two-electron components, there may also exist electron beams streaming along the magnetic field.[1,11,12] It is suggested that the electrostatic waves excited in such a plasma system, composed of cold, hot, and beam electrons, may explain the broadband electrostatic noise (BEN) observed in the Earth's auroral region. On the basis of a linear theory, Tokar and Gary[1] found that the electron-acoustic mode is unstable in such a case. Lin *et al.*[13] investigated the temporal behavior of this instability with numerical simulations, and demonstrated that the instability saturates due to either the trapping of electrons or the forming of a plateau on the velocity distribution of the beam electrons. Matsukiyo *et al.*[14] found that, in addition to the electron-acoustic waves, the Langmuir waves are also excited by the electron beam, and, according to their study, the Langmuir waves are more important than the electron-acoustic waves. Using a KdV equation, Berthomier *et al.*[15] presented the solution of solitary structures in such a beam-plasma system, and the solitary structures have positively charged potentials. However, Lu *et al.*[16] demonstrated with a one-dimensional (1D) electrostatic particle-in-cell (PIC) simulations that the solitary structures with positive charged potentials are formed in such a plasma system.

In this paper, we perform 1D PIC electrostatic simulations to investigate the nonlinear evolution of the electrostatic waves excited in an unmagnetized plasma, which consists of three-electron components: cold, hot, and beam electrons. We also try to investigate the different electrostatic waves with different parameters. The conditions that lead to

TABLE I. Simulation parameters for Run 1–11.

Run	$\alpha=n_{h0}/n_{c0}$	$\beta=n_{b0}/n_{c0}$	$\theta=T_h/T_c$	$\varphi=T_h/T_b$	u_d/v_{Tc}
1	1.0	0.04	100.0	100.0	20.0
2	1.0	0.04	100.0	100.0	15.0
3	1.0	0.04	100.0	100.0	8.0
4	8.8	0.20	100.0	100.0	20.0
5	0.011	0.002	100.0	100.0	20.0
6	1.0	0.04	50.0	50.0	20.0
7	1.0	0.04	10.0	10.0	20.0
8	1.0	0.04	100.0	10.0	20.0
9	1.0	0.04	100.0	1.0	20.0
10	1.0	0.02	100.0	100.0	20.0
11	1.0	0.10	100.0	100.0	20.0

the formation of solitary structures through nonlinear evolution are also discussed.

The paper is organized as follows. In Sec. II, we describe the 1D electrostatic PIC simulation code. The simulation results are presented in Sec. III. The discussion and conclusions are given in Sec. IV, and the significance of the simulation results to the auroral observations is also discussed in this section.

II. SIMULATION MODEL

A 1D electrostatic PIC code with periodic boundary conditions is employed in our simulations.[17] This simulation model neglects the effect of the ambient magnetic field. In this code ions are motionless and form a neutralizing background. Essentially we consider three-electron components: cold, hot, and beam electrons. The initial velocity distributions of the three-electron components are assumed to be Maxwellian, and the streaming electrons have a beam speed. The unperturbed densities of the cold, hot, and beam electrons are n_{c0}, n_{h0}, and n_{b0}, respectively, while their temperatures are $T_c(v_{Tc})$, $T_h(v_{Th})$, and $T_b(v_{Tb})$. The beam speed of beam electrons is denoted by u_d, and the total unperturbed density is $n_0=n_{c0}+n_{h0}+n_{b0}$. In the simulations, the densities and velocities of the electrons are expressed in units of the total unperturbed density n_0 and thermal velocity of cold electrons v_{Tc}, respectively. The space and time (x and t) are normalized to the cold electron Debye length $\lambda_{Dc}=(\varepsilon_0 k_B T_c/n_{c0}e^2)^{1/2}$ and to the inverse of the total electron plasma frequency $\omega_{pe}=(n_0e^2/m_e\varepsilon_0)^{1/2}$. The electric field and potential are normalized to $m_e\omega_{pe}v_{Tc}/e$ and $k_BT_c/e\varepsilon_0$. Grid cells (1024) with grid size $1.0\lambda_{Dc}$ are used in the simulations, and the time step is $0.02\omega_{pe}^{-1}$. The number of particles employed for each component of electrons is 409 600. In addition, for convenience, we introduce the following quantities to be used in the subsequent study:

$$\alpha=\frac{n_{h0}}{n_{c0}}, \quad \beta=\frac{n_{b0}}{n_{c0}}, \tag{2}$$

$$\theta=\frac{T_h}{T_c}, \quad \varphi=\frac{T_h}{T_b}. \tag{3}$$

III. SIMULATION RESULTS

We perform a parameter survey of the excited electrostatic waves in the beam-electron plasma system composed of cold, hot, and beam electrons. In such a plasma system, the linear dispersion relation takes the following form:

$$1+\frac{2}{k^2\lambda_{Dc}^2}[1+\zeta_c Z(\zeta_c)]+\frac{2}{k^2\lambda_{Dh}^2}[1+\zeta_h Z(\zeta_h)]+\frac{2}{k^2\lambda_{Db}^2}[1+\zeta_b Z(\zeta_b)]=0, \tag{4}$$

where $\zeta_c=\omega/kv_{Tc}$, $\zeta_h=\omega/kv_{Th}$, and $\zeta_b=(\omega-ku_d)/kv_{Tb}$. $Z(\zeta)=1/\sqrt{\pi}\int_{-\infty}^{\infty}[\exp(-x^2)]/(x-\zeta)dx$ is the usual plasma dispersion function. λ_{Dc}, λ_{Dh}, and λ_{Db} are the Debye lengths of the cold, hot, and beam electrons, respectively. If the effect of beam electrons can be neglected ($n_b \ll n_0$), and if we consider $\zeta_h<1$, Eq. (4) reduces to Eq. (1), which is the dispersion relation of the electron-acoustic waves. On the other hand in case of $\zeta_h>1$, Eq. (4) may be approximated as[18]

$$\omega^2=\omega_{pc}^2(1+3k^2\lambda_{Dc}^2)+\omega_{ph}^2(1+3k^2\lambda_{Dh}^2), \tag{5}$$

which represents the Langmuir-wave dispersion relation. Besides these two modes, there exists another wave mode: the beam-driven electrostatic waves. When the streaming speed of the beam electrons is sufficiently large, the dispersion relation of this wave mode can be approximated as

$$1-\frac{\omega_{pc}^2}{\omega^2}-\frac{\omega_{ph}^2}{\omega^2}-\frac{\omega_{pb}^2}{(\omega-ku_d)^2}=1, \tag{6}$$

where ω_{pc}, ω_{ph}, and ω_{pb} are the electron plasma frequency of the cold, hot, and beam electrons, respectively. One solution of this dispersion equation is the beam-driven wave mode, which can be expressed with the following equation when $n_b \ll n_0$:[18]

$$\omega=\frac{ku_d}{1+n_b/n_0}\approx ku_d. \tag{7}$$

The details of this wave mode can be found in Ref. 18. In this section, a comparative study of the three electrostatic wave modes is presented. The parameters of the cases studied are listed in Table I.

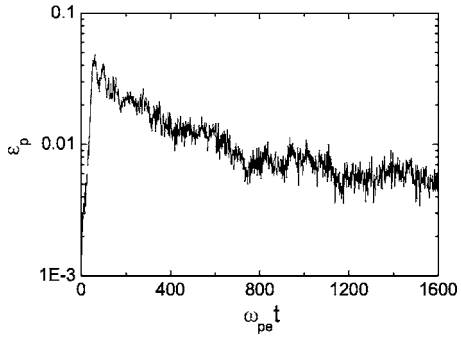

FIG. 1. The time evolution of the normalized electric field energy $\varepsilon_p = \varepsilon_0 E^2/(2n_0 k_B T_c)$ in logarithmic scale for Run 1.

A. Analysis of the reference case

In the simulations, Run 1 is chosen as the reference case, and Fig. 1 shows its time evolution of the normalized electric field energy $\varepsilon_p = \varepsilon_0 E^2/(2n_0 k_B T_c)$ in logarithmic scale. It first passes through a linear growth stage and saturates at $\omega_{pe}t \sim 50.0$. At last it reaches a quasiequilibrium stage at $\omega_{pe}t \sim 1000.0$. At this stage the electric field energy remains nearly constant.

In Fig. 2, we present an ω-k diagram, which is obtained by Fourier transforming the electric field E_x in space and time. In this figure, $\omega_{pe}t=0-51.2$ and $\omega_{pe}t=1200-1251.2$ correspond to the linear growth and quasiequilibrium stages, respectively. Obviously, the electron-acoustic waves, Langmuir waves and beam-driven electrostatic waves, whose dispersion relations are given in Eqs. (1), (5), and (6), respectively, are excited. The frequencies of the electron-acoustic waves are around the cold electron plasma frequency $\omega_{pc} = 0.7\omega_{pe}$. The Langmuir waves are very weak due to Landau damping caused by the hot electrons. The beam-driven waves dominate the wave spectrum, and they have a broad frequency spectrum with phase speed about the beam speed. In the linear growth stage this broad frequency spectrum extends from about $0.5\omega_{pe}$ to $2.0\omega_{pe}$. However, in the nonlinear stage its spectrum drifts to lower frequency, which extends from about $0.1\omega_{pe}$ to $1.5\omega_{pe}$. The reason is attributed to electron trapping. It should be noted that the dispersion relations plotted in the figure are based on parameters of the unperturbed plasma. However, the excitation of the waves can affect these parameters. As a result, there are discrepancies

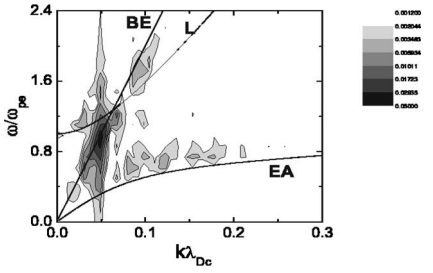

FIG. 2. The $\omega-k$ spectra at $\omega_{pe}t=0-51.2$ and $\omega_{pe}t=1200-1251.2$ for Run 1. In this and following ω-k spectra, L, EA, and BE denote dispersion relations of the Langmuir, electron-acoustic, and beam-driven wave modes, respectively.

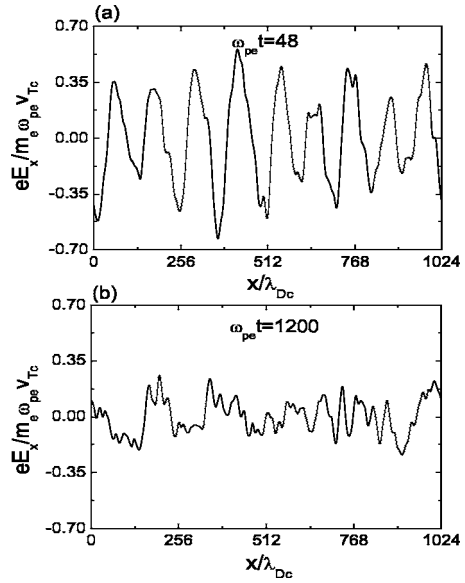

FIG. 3. (a) The spatial profiles of the electric field E_x at (a) $\omega_{pe}t=48.0$ and (b) $\omega_{pe}t=1200.0$ for Run 1.

between the expected dispersion relations and those reflected in our results. Figure 3 displays the spatial profiles of the electric field E_x at different times, and Fig. 4 depicts the x-v_x phase-space plots for the beam, cold, and hot electrons.

In the figure, $\omega_{pe}t=48.0$ and $\omega_{pe}t=1200.0$ correspond to the linear growth and quasiequilibrium stage, respectively. In the linear growth stage, the nearly monochromatic electrostatic waves can trap the beam electrons and form the characteristic vortex pattern in phase space. In the nonlinear evolution stage, the beam electrons are mixed in phase space, which obscures the effect of trapping and results in heating of the beam electrons. At the same time, the cold and hot electrons are also heated by the enhanced waves. These combined effects lead to the saturation of the waves excited.

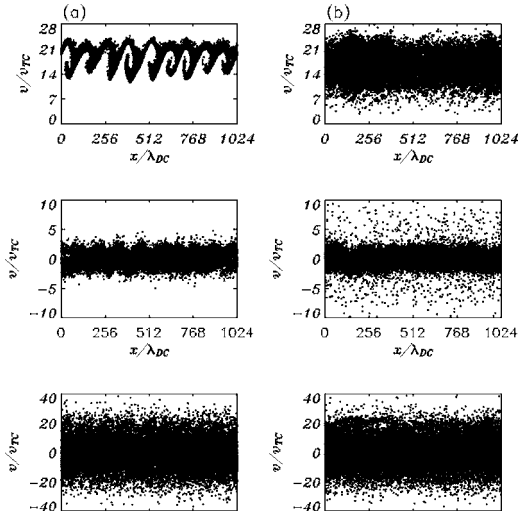

FIG. 4. The x-v_x phase-space plots for the beam, cold, and hot electrons at (a) $\omega_{pe}t=48.0$ and (b) $\omega_{pe}t=1200.0$ for Run 1.

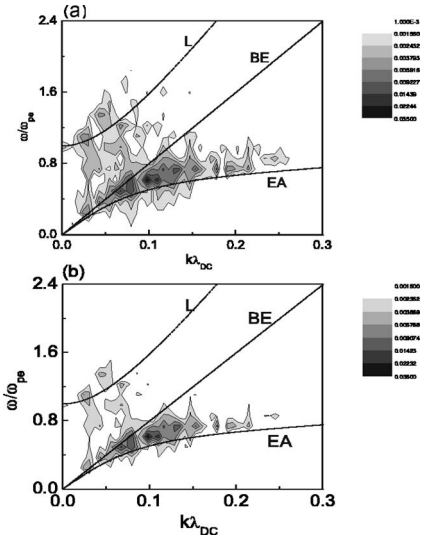

FIG. 5. The ω-k spectra at $\omega_{pe}t=1200-1251.2$ for (a) Run 2 and (b) Run 3.

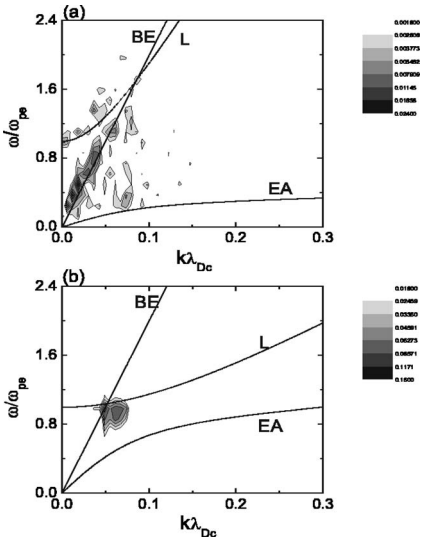

FIG. 6. The $\omega-k$ spectra at $\omega_{pe}t=1200-1251.2$ for (a) Run 4 and (b) Run 5.

B. The effects of the drift speed of the electron beam

Here we change the speed of the electron beam but let other parameters be the same as in the reference case (Run 1). We see that the time evolution of the excited electric field energy and the heating of the three-electron components are similar. The most interesting effect occurs in the wave spectrum. Figure 5 is for Run 2 and Run 3 at the quasiequilibrium stage. The speeds of the electron beam are $u_d=15.0v_{Tc}$ and $u_d=8.0v_{Tc}$ in Run 2 and Run 3, respectively. It is shown that decreasing the beam speed tends to reduce the amplitude of the beam-driven waves. Consequently, the electron-acoustic wave mode becomes increasingly more important. In Run 3, for the drift speed of the electron beam $u_d=8.0v_{Tc}$, the beam-driven waves vanish, while the electron-acoustic waves become the dominant mode. Detailed investigations show that the electron-acoustic waves tend to take over in the case where the beam speed u_d becomes below the thermal velocity of the hot electrons. The reason is that when the phase speed of beam-driven waves decreases, Landau damping dominates.

C. The effects of hot to cold electron density ratio

The hot to cold electron density ratio also has an important effect on the excited waves. We now change the hot to cold density ratio α, while keep the density of electron beam $n_b=0.02n_0$. Moreover, we also change the beam to cold electron density ratio β. The ω-k plots of Run 4 and Run 5 at the quasiequilibrium stage are shown in Fig. 6. The increase of the hot electron density tends to enhance the beam-driven wave and Langmuir waves. This point is demonstrated in Fig. 6(a). It is shown that the electron-acoustic waves are very weak. Actually, when the cold electron vanishes the electron-acoustic waves also disappear. Figure 6(b) shows that only the Langmuir waves exist. This means increasing the cold electron density can enhance the amplitude of the Langmuir waves and reduce the amplitude of the beam-driven waves and electron-acoustic waves. In this situation, the Landau damping of the Langmuir waves decreases with the decrease of the density of the hot electrons.

D. The effects of the hot electron temperature

Here we investigate the effect of the hot electron temperature on the properties of the excited waves. In reference to Run 1, we only change the hot electron temperature. The ω-k plots of the excited waves for Run 6 and Run 7 are presented in Fig. 7. It is found that a decrease of the hot electron temperature tends to reduce the amplitude of the beam-driven waves and electron-acoustic waves. At the same time, it increases the amplitude of the Langmuir waves due to decreased Landau damping. In Fig. 7(b), for $\theta=\varphi=10.0$, the Langmuir waves become the only existing wave mode.

E. The effects of the beam electron temperature

Here we study the influence of the beam electron temperature on the excited waves, while keeping other param-

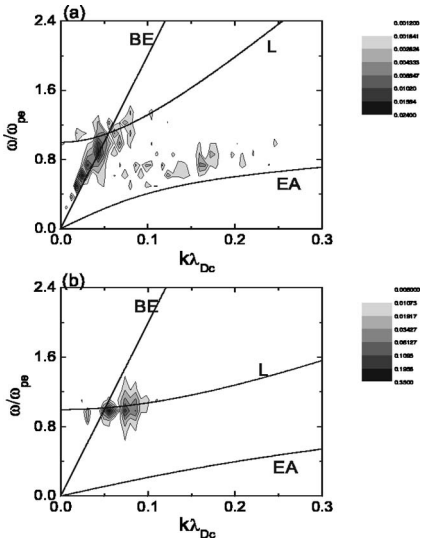

FIG. 7. The ω-k spectra at $\omega_{pe}t=1200-1251.2$ for (a) Run 6 and (b) Run 7.

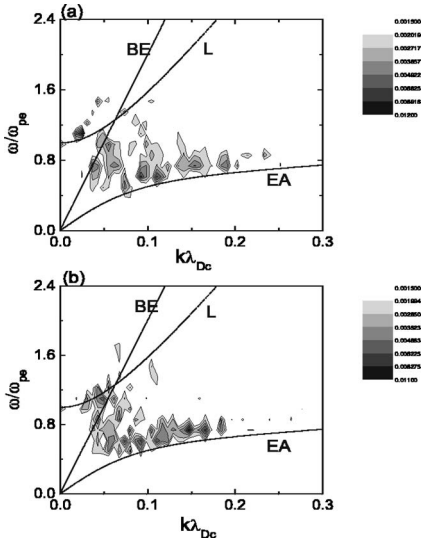

FIG. 8. The ω-k spectra at $\omega_{pe}t=1200-1251.2$ for (a) Run 8 and (b) Run 9.

eters used in the reference case (Run 1) unchanged. Figure 8 shows the ω-k plots of the excited waves in Run 8 and Run 9. In Run 8, the beam electron temperature is ten times that of the cold electron temperature and $\varphi=10.0$. The amplitude of electron-acoustic wave is obviously larger than that of the beam-driven waves. This trend is observed more clearly in Run 8, when the beam electron temperature is 100 times that of the cold electron temperature. As pointed out in the reference case, the beam-driven waves saturate due to the heating of the beam electrons. Therefore, increasing the beam electron temperature will reduce the amplitude of the beam-driven electrostatic mode.

F. The effects of the beam electron density

We now change the beam electron density, but keep the cold and hot electrons at the same density. Figure 9 presents the ω-k plot of the excited waves at $\omega_{pe}t=1200.0$ for $n_b \approx 0.01n_0$ (Run 10) and $n_b \approx 0.05n_0$ (Run 11). In comparison with the reference case, increase of the beam electron density tends to enhance the amplitude of the beam-driven mode. In the case $n_b=0.05n_0$, the amplitude of the beam-driven waves is much higher than those of other modes. This leads to the formation of the solitary waves. Figure 10 shows the electric field E_x and electric potential ψ at $\omega_{pe}t=1200.0$ for Run 11. It is seen that the electric field has two bipolar structures with positive potentials. They are compressive solitary waves. In the x-v_x phase diagram of the three-electron components at the quasiequilibrium stage (shown in Fig. 11), we find that there are phase-space holes at the position of the solitons for the beam electrons. So, the solitons are of the Bernstein-Greene-Kruskal (BGK) wave mode that is attributed to electron phase-space holes due to the trapped electrons in the potential wells.[19–22] The generation process of these solitons was previously discussed in Refs. 16, 23, and 24.

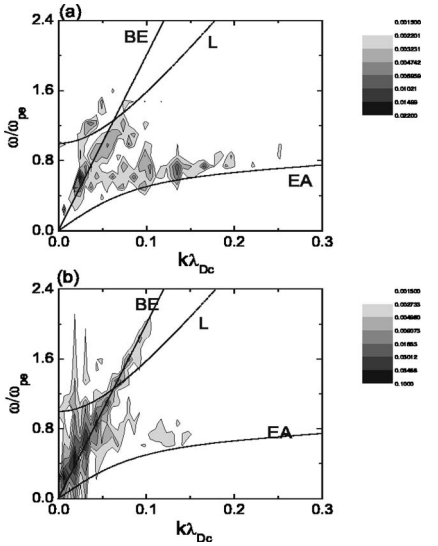

FIG. 9. The ω-k spectra at $\omega_{pe}t=1200-1251.2$ for (a) Run 10 and (b) Run 11.

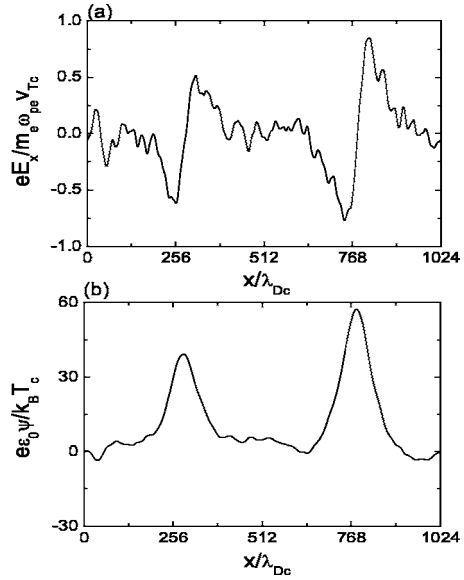

FIG. 10. The spatial profiles of electric field E_x and potential ψ at $\omega_{pe}t=1200.0$ for Run 11.

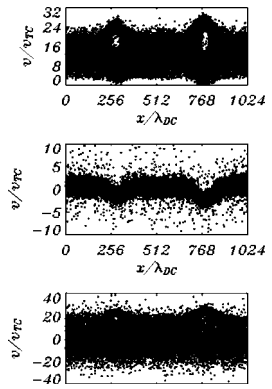

FIG. 11. The x-v_x phase-space plots for the beam, cold, and hot electrons at $\omega_{pe}t=1200.0$ for Run 11.

IV. DISCUSSIONS AND CONCLUSIONS

In this paper, we report the result of a 1D electrostatic PIC simulation that aims to investigate waves excited by an electron beam in a plasma with hot and cold electron components. It is observed that such a plasma system is unstable to electrostatic waves with frequencies in the range of broadband electrostatic noise in the auroral region. Tokar and Gary[1] first pointed out that the electron-acoustic waves can be excited by the electron beam. Later Lin *et al.*[13] studied the linear and nonlinear behaviors of the beam-driven electron-acoustic instability with PIC simulations, and these authors showed that the instability saturates by trapping the electrons or forming a plateau on the velocity distributions of the beam electrons. Matsukiyo *et al.*[14] found that the Langmuir waves as well as the electron-acoustic waves can be excited by the electron beam in such a plasma system. In the studies of both Lin *et al.* and Matsukiyo *et al.*, the temperature of the beam electrons is considered to be much higher than that of the cold electrons.

In this paper we present a comparative study of the electrostatic waves excited in the beam-plasma system. Three wave modes are unstable in such a plasma system. Besides the Langmuir waves and electron-acoustic waves, there still exists the third wave mode: the beam-driven electrostatic waves. It has a very broad frequency spectrum, which can extend from about $(0.1-0.2)\omega_{pe}$ to $(1.5-2.5)\omega_{pe}$, and its phase speed is about that of the streaming speed of the electron beam. The excitation condition for this third wave mode is when there exists a drift speed between a cold electron beam and thermal background hot electrons. The Langmuir waves only dominate the situation when the density or temperature of the hot electrons is small, while the electron-acoustic waves become dominant when the speed of the electron beam is sufficiently low or the temperature of the beam electrons is sufficiently high. The increase of the streaming speed and density of the beam electrons or the increase of the density and temperature of the hot electrons tends to make the beam-driven waves take control over the wave spectrum. Compressive solitary waves with a bipolar structure of electric fields are formed when the density of beam electrons is sufficiently high. The formation mechanisms and characteristics of the solitary waves are similar to the situations investigated by Omura *et al.*[23,24] Actually such large amplitude solitary wave structures are recently observed in the auroral region with the POLAR and FAST satellites.[25–28] Generally these structures have positively charged potentials and propagate along the ambient magnetic field.

Intense electric field noise along the auroral field line has been observed in the auroral region.[12,29,30] Such intense and impulsive broadband electrostatic noise has also been revealed by the Viking satellite in which the high temporal resolution wave experiments show the following characteristics:[31,32] The impulsive emission has amplitude up to 100 mV/m and variation time a few hundreds of milliseconds. The spectrum of wave power can extend from very low frequencies up to frequencies much higher than the generally assumed local electron plasma frequency. In our study, the frequencies of the electrostatic waves excited in the beam-plasma system extend from 0.1 to 2.5 times of the local electron plasma frequency, which may explain a part of BEN spectrum.

ACKNOWLEDGMENTS

The authors thank C. S. Wu at the University of Maryland for a helpful discussion. This research was supported by the National Science Foundation of China (NSFC) under Grant Nos. 40336052, 40304012, 40404012, and the Chinese Academy of Sciences, under Grant No. KZCX3-SW-144.

[1] R. L. Tokar and S. P. Gary, Geophys. Res. Lett. **11**, 1180 (1984).
[2] R. L. Mace and M. A. Hellberg, J. Plasma Phys. **43**, 239 (1990).
[3] R. L. Mace, S. Baboola, R. Bharuthram, and M. A. Hellberg, J. Plasma Phys. **45**, 323 (1991).
[4] A. A. Mamun, P. K. Shukla, and L. Stenflo, Phys. Plasmas **9**, 1474 (2002).
[5] B. D. Fried and R. W. Gould, Phys. Fluids **4**, 139 (1961).
[6] K. Watanabe and T. Taniuti, J. Phys. Soc. Jpn. **43**, 1819 (1977).
[7] S. P. Gary and R. L. Tokar, Phys. Fluids **28**, 2439 (1985).
[8] N. Dulouloz, R. Pottelette, M. Malingre, and R. A. Treumann, Geophys. Res. Lett. **18**, 155 (1991).
[9] N. Dulouloz, R. A. Treumann, R. Pottelette, and M. Malingre, J. Geophys. Res. **98**, 17415 (1993).
[10] R. L. Mace and M. A. Hellberg, Phys. Plasmas **8**, 2649 (2001).
[11] R. Pottelette, R. E. Ergun, R. A. Treumann, M. Berthomier, C. W. Carlson, J. P. McFadden, and I. Roth, Geophys. Res. Lett. **26**, 2629 (1999).
[12] C. S. Lin, J. L. Burch, S. D. Shawhan, and D. A. Gurnett, J. Geophys. Res. **89**, 925 (1984).
[13] C. S. Lin, D. Winske, and R. Tokar, J. Geophys. Res. **90**, 8269 (1985).
[14] S. Matsukiyo, R. A. Treumann, and M. Scholar, J. Geophys. Res. **109**, A06212 (2004).
[15] M. Berthomier, R. Pottelette, M. Malingre, and Y. Khotyaintsev, Phys. Plasmas **7**, 2987 (2000).
[16] Q. M. Lu, D. Y. Wang, and S. Wang, J. Geophys. Res. **110**, A03223 (2005).
[17] Q. M. Lu and D. S. Cai, Comput. Phys. Commun. **135**, 93 (2001).
[18] R. A. Treumann and W. Baumjohann, *Advanced Space Plasma Physics* (Imperial College Press, London, 1997).
[19] M. V. Goldman, M. M. Oppenheim, and D. L. Newman, Geophys. Res. Lett. **26**, 1821 (1999).
[20] L. Muschietti, R. E. Ergun, I. Roth, and C. W. Carlson, Geophys. Res. Lett. **26**, 1093 (1999).
[21] M. M. Opphenheim, D. L. Newman, and M. V. Goldman, Phys. Rev. Lett. **83**, 2344 (1999).
[22] M. M. Opphenheim, G. Vetoulis, D. L. Newman, and M. V. Goldman, Geophys. Res. Lett. **28**, 1891 (2001).
[23] Y. Omura, H. Kojima, and H. Matsumoto, Geophys. Res. Lett. **21**, 2923 (1994).
[24] Y. Omura, H. Matsumoto, T. Miyake, and H. Kojima, J. Geophys. Res. **101**, 2685 (1996).
[25] J. R. Franz, P. W. Kintner, and J. S. Pickett, Geophys. Res. Lett. **25**, 1277 (1998).
[26] B. T. Tsurutani, J. K. Arballo, G. S. Lakhina *et al.*, Geophys. Res. Lett. **25**, 4117 (1998).
[27] R. E. Ergun, C. W. Carlson, J. P. McFadden *et al.*, Geophys. Res. Lett. **25**, 2041 (1998).
[28] C. A. Cattell, J. Dombeck, J. R. Wygant *et al.*, Geophys. Res. Lett. **26**, 425 (1999).
[29] D. A. Gurnett and L. A. Frank, J. Geophys. Res. **82**, 1031 (1977).
[30] D. A. Gurnett and U. S. Inan, Rev. Geophys. **26**, 285 (1988).
[31] R. Pottelette, M. Malinger, A. Bahnsen, L. Eliasson, K. Stasiewicz, R. E. Erlandson, and G. Marklund, Ann. Geophys. **6**, 573 (1988).
[32] R. Pottelette, M. Malingre, N. Dobouloz, B. Aparicio, R. Lundin, and G. Marklund, J. Geophys. Res. **95**, 5957 (1990).